Tampere University

Risto-Matti Hoikka

COMPARISON OF AUTOMATED VEHICLE STEERING CONTROL METHODS

Bachelor's thesis
Faculty of Engineering and Natural Sciences
Examiner: Veli-Pekka Pyrhönen
January 2024

ABSTRACT

Risto-Matti Hoikka: Comparison of automated vehicle steering control methods
Bachelor's thesis
Tampere University
Automation engineering
January 2024

This thesis investigates control systems and steering models that are used to control steering of the automated vehicles. The aim of the study is to gain insight into the current control system of the research vehicle, to identify its basic challenges and to look for areas of improvement. Although automated driving is undergoing continuous technological advancements, the nonlinearity of the system and other challenges complicate the design process, making it difficult to find a single optimal solution.

The work is divided into two parts: a theoretical part and an experimental part. The theoretical part covers various types of controllers as well as dynamic and kinematic models. The use of models enables to study properties of the system under investigation and the design of the control system. Therefore, it is important to obtain the most suitable model for design purposes. In addition, the theoretical part of the thesis discusses different performance measures that can be used to study the performance of a closed-loop control system. These performance indices focus on the calculation of error accumulation in different ways, which makes them well suited to study the servo performance of the control system.

Control systems are often based on negative feedback, where the measured output is fed back to the input and then the error is calculated. With the error, the controller generates a control signal that controls the system and tries to mitigate the error between the setpoint and the measurement. Therefore, the limitations and uncertainties of the measurement and control system must be taken care of as well as possible. In the theoretical part, the sensors and hardware of the automated driving system are discussed and the constraints they impose are examined.

The experimental part presents the measurements carried out with the three different types of controllers. In the experimental part the performance of the control system was evaluated using P (Proportional), PI (Proportional-Integral), and PID (Proportional-Integral-Derivative) controllers. The results showed that the best performance was achieved with P and PI controllers. The PID controller caused significant oscillation in the vehicle steering, which resulted in poorest performance in the controller comparison.

Keywords: Steering control, autonomous driving, PID controller, control theory

TIIVISTELMÄ

Risto-Matti Hoikka: Automatisoidun ajoneuvon ohjauksen säätötapojen vertailu
Kandidaatin työ
Tampereen yliopisto
Automaatiotekniikka
Tammikuu 2024

Tässä työssä keskitytään automatisoitujen ajoneuvojen ohjaamiseen käytettyjen mallien ja säätömenetelmien tarkasteluun. Tutkimuksen päämääränä on syventyä testiajoneuvon nykyiseen säätöjärjestelmään, tunnistaa sen haasteet ja etsiä kehityskohteita, joilla järjestelmää voitaisiin kehittää. Tällä hetkellä automatisoitu ajaminen kehittyy teknisesti jatkuvasti, mutta järjestelmän epälineaarisuus ja muut haasteet hankaloittavat suunnitteluprosessia eikä automaattiseen ajamiseen ole yhtä oikeaa ratkaisua löydettävissä.

Työ on jaettu kahteen osaan: teoriaosuuteen ja kokeelliseen osuuteen. Teoriaosuudessa käsitellään erilaisia säädintyyppejä sekä dynaamisia ja kineettisiä malleja. Mallien käyttö helpottaa tutkittavan systeemin ominaisuuksien tutkimista sekä säädinsuunnittelua, minkä vuoksi mahdollisimman sopivan mallin saaminen on tärkeää. Lisäksi teoriaosuudessa käsitellään erilaisia hyvyyslukuja, joilla voidaan tutkia säätöjärjestelmän suorituskykyä. Kyseiset hyvyysluvut keskittyvät virheen kertymisen laskemiseen erilaisin tavoin, jonka vuoksi ne soveltuvat hyvin tämän työn säätöjärjestelmän servotehtävän hyvyyden tutkimiseen.

Säätöjärjestelmät perustuvat usein negatiiviseen takaisinkytkentään, jossa asetusarvosta vähennetään ulostulon mittaus. Tätä kutsutaan erosuureeksi, joka muodostetaan säätimessä. Erosuureen avulla säädin muodostaa ohjaussignaalin, joka säätää järjestelmää ja pyrkii pienentämään asetusarvon ja mittauksen välisen virheen. Tämän vuoksi mittaus – ja ohjausjärjestelmän rajoitteet ja epävarmuudet on tunnettava mahdollisimman hyvin. Teoriaosuudessa arvioitiin automaattisen ajoneuvon antureita ja laitteistoa sekä tutkitaan näiden aiheuttamia rajoitteita.

Kokeellisessa osuudessa esitellään kolmella eri säädintyypillä suoritetut mittaukset ja niiden tulokset. Tutkimuksen kokeellisessa osuudessa arvioitiin säätöjärjestelmän suorituskykyä käyttäen P- (Proportional), PI- (Proportional-Integral), ja PID (Proportional-Integral-Derivative) -säätimiä. Tulosten perusteella havaittiin, että parhaimmat suoritusominaisuudet saavutettiin P- ja PI-säätimillä. PID-säätimen käyttö aiheutti ajoneuvon ohjaukseen merkittävää värähtelyä, joka johti sen heikkoon suorituskykyyn säädinvertailussa.

Avainsanat: Ajoneuvon ohjauksen säätö, autonominen ajaminen, PID-säädin, säätötekniikka

PREFACE

This work was done for VTT, and I would like to thank the whole Automated Vehicles research team for making the work possible, and for their help during the work. I particularly want to thank M.Sc. Topi Miekkala for his constructive feedback and guidance during the process.

I would also like to thank my examiner Veli-Pekka Pyrhönen from the University of Tampere for his comments and feedback, which helped to complete this thesis.

Tampere, 22 January 2024

Risto-Matti Hoikka

CONTENTS

LIST OF SYMBOLS AND ABBREVIATIONS

1-DOF	1-Degree-of-Freedom
2-DOF	2-Degree-of-Freedom
3-DOF	3-Degree-of-Freedom
9-DOF	9-Degree-of-Freedom
CAN	Controller Area Network
DDS	Data-Distributed System
GNSS	Global Navigation Satellite System
IAE	Integral of Absolute Error
IMU	Inertial Measurement Unit
ISE	Integral of Squared Error
ITAE	Integral of Time multiplied Absolute Error
ITSE	Integral of Time multiplied Square Error
LTI	Linear-Time-Invariant
PID	Proportional-Integral-Derivative
$\boldsymbol{A}$	Dynamic matrix of the state-space representation
$\boldsymbol{A}_{cl}$	Dynamic matrix of the feedback system
$\boldsymbol{B}$	Input matrix of the state-space representation
$\boldsymbol{C}$	Output matrix of the state-space representation
$C_{\alpha f}$	Cornering stiffness value of the front tires
$C_{\alpha r}$	Cornering stiffness value of the rear tires
$\boldsymbol{D}$	Direct transfer matrix of the state-space representation
$\boldsymbol{I}$	Identity matrix
I_z	Moment around z-axis
$\boldsymbol{K}$	Gain matrix
K_p	Proportional gain
T	Time period of the integral
T_d	Derivative time
T_i	Integration time
V_x	Longitudinal velocity of the vehicle of the dynamic bicycle model
$\dot{X}$	Horizontal velocity of the kinematic bicycle model
$\dot{Y}$	Vertical velocity of the kinematic bicycle model

$e(t)$	Error signal
h	Sampling interval
l_f	Length from the vehicle's centre of mass to the front
l_r	Length from the vehicle's centre of mass to the rear
m	Mass of the vehicle
$r(t)$	Reference value
$u(t)$	Control signal of PID controller
$\boldsymbol{u}(t)$	m-dimensional input vector of the state space representation
$\boldsymbol{x}(t)$	*n*-dimensional state vector of the state space representation
$\dot{\boldsymbol{x}}(t)$	n-dimensional first-order time derivative of $\boldsymbol{x}(t)$ of the state space representation
$y(t)$	Output of the system
$\boldsymbol{y}(t)$	r-dimensional output vector of the state space representation
$\dot{y}$	Lateral velocity of the vehicle of the dynamic bicycle model
$\ddot{y}$	Lateral acceleration of the vehicle of the dynamic bicycle model
β	Slip angle
$\boldsymbol{\lambda}$	Eigenvalue vector
$\dot{\psi}$	Yaw angular velocity
$\ddot{\psi}$	Yaw angular acceleration

1. INTRODUCTION

In recent years, there has been a significant increase in research on autonomous driving. Autonomous systems are based on complex control and decision-making technologies that allow vehicles to move safely and efficiently without a human driver [1]. A key part of this technology is the control of the steering of a self-driving car, which allows the car to control and adapt to changes in the environment in real time.

Self-driving car steering control covers a wide range of methods and strategies used to control the movement of the car in different situations. Control systems can be based on traditional control theory methods or deep machine learning algorithms and must be able to react quickly to changing environmental factors. [2]

Steering control is an essential part of the implementation of autonomous driving, aiming to achieve optimal performance and safety in different traffic situations [2]. At the same time, vehicle modelling provides the basis for steering control, as an accurate modelling of vehicle dynamics is essential for optimal steering design.

Vehicle modelling is another key aspect of autonomous driving research. An accurate and realistic vehicle model allows experimentation and testing in simulation environments without the need for a physical vehicle. Modelling involves challenges such as the complexity of vehicle dynamics and the variability of the environment. [1]

Various control methods have been used to control the lateral steering of the vehicle. For example, gain-scheduling, model-based control and neural network-based controllers have been developed for automated vehicles. Each control method has its own advantages, such as operating over large speed ranges or at large turning angles. On the other hand, some methods can be difficult to implement, but are robust and efficient. [3][4][5]

The purpose of this thesis is to examine the different types of vehicle motion models and control methods for lateral vehicle motion. Additionally, the work examines how an automatic car behaves with three different controllers and uses this information to provide suggestions for improvements to the current system. The controllers to be considered are the P (Proportional), PI (Proportional-Integral) and PID (Proportional-Integral-Derivative) controllers. However, not everything related to the research vehicle and technology will be examined for confidentiality reasons.

The thesis describes the underlying theory behind the steering of the autonomous vehicles. Chapter 2 discusses the control of the steering of a self-driving car and the control models. Chapter 3 discusses the research vehicle and the implementation of the field test. Finally, Chapter 4 presents the results of the measurements that describe the performance of the P, PI, and PID controllers.

2. STEERING CONTROL

One of the most significant challenges encountered within the realm of autonomous driving steering control pertains to the nonlinearity inherent in steering systems. Different steering models and controllers have been developed and each of them has different features. Certain methods exhibit good performance during low-speed manoeuvres and cornering scenarios, while others demonstrate effectiveness when addressing high-speed situations and executing minor turns.

2.1 Steering models

The vehicle's motion can be explained through either more complex four-wheel models or simplified two-wheel bicycle models. Within the bicycle model, the four-wheel configuration is substituted with a dual-tire arrangement comprising a front and a rear tire. Moreover, two distinct classifications of models exist: dynamic and kinematic. Each of these models have uses in different scenarios. [6, p. 20]

Mathematical models

Steering models can be described in various ways. In this thesis, models are presented using time-depend differential equations. A differential equation is an equation that includes a function and its derivatives. These equations are especially valuable for modelling dynamic phenomena, such as car's steering. [7, p. 724]

State-space representation is a method used to express differential equations, and it can be used to monitor how states evolve over time. The Linear Time Invariant (LTI) state-space representation can be expressed in the form of equation

$$\begin{aligned} \dot{\boldsymbol{x}}(t) &= \boldsymbol{A}\boldsymbol{x}(t) + \boldsymbol{B}\boldsymbol{u}(t) \\ \boldsymbol{y}(t) &= \boldsymbol{C}\boldsymbol{x}(t) + \boldsymbol{D}\boldsymbol{u}(t)\,' \end{aligned} \tag{1}$$

where $\boldsymbol{x}(t)$ is n-dimensional state vector, $\dot{\boldsymbol{x}}(t)$ is n-dimensional first-order time derivative of $\boldsymbol{x}(t)$, $\boldsymbol{u}(t)$ is m-dimensional input vector and $\boldsymbol{y}(t)$ is r-dimensional output vector. [8, p. 12] A system is an LTI system when it is time invariant and adheres the superposition principle. The superposition principle holds when each input u_n produces an output y_n and these outputs are not dependent on other inputs. [9, p. 87] Other elements of the state-space representation are matrices $\boldsymbol{A} \in \mathbb{R}^{n\times n}$, $\boldsymbol{B} \in \mathbb{R}^{n\times m}$, $\boldsymbol{C} \in \mathbb{R}^{r\times n}$ and $\boldsymbol{D} \in \mathbb{R}^{r\times m}$. Specifically, matrix ***A*** is the dynamic matrix, matrix ***B*** is the input matrix, matrix ***C*** is the output matrix, and matrix ***D*** is the direct transfer matrix. Of these matrices, matrix ***A*** is the most relevant when describing vehicle lateral control models. Matrix ***B*** defines which

states are controlled, matrix ***C*** describes which states are measured and matrix ***D*** describes which inputs affects directly to the output of the system. [8, p. 12]

Kinematic bicycle model

Kinematic model has been derived based on geometric relationships of the vehicle without any forces. This approach has proven applicable and robust in situations where precise dynamic parameters are unavailable, or the identification of the model is too complicated. Kinematic bicycle model is illustrated in Figure 1.

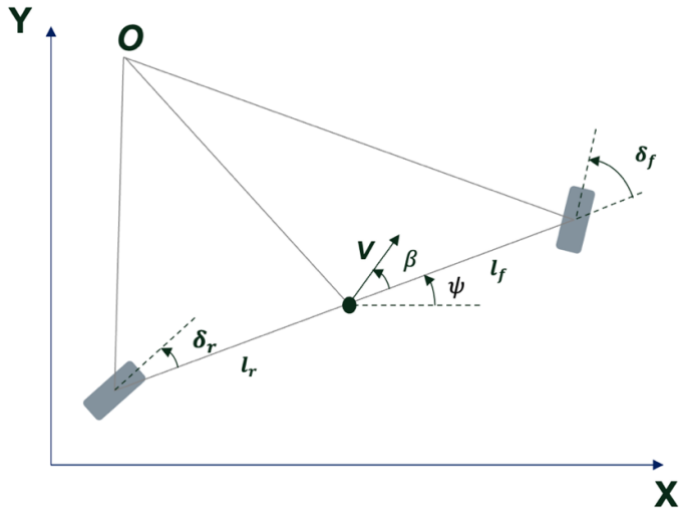

Figure 1. *Vehicle's kinematic motion. Edited from source.* [6, p. 21]

Based on Figure 1, differential equations of the vehicle's kinematic motion can be derived from

$$\begin{cases} \dot{X} = V\cos(\psi+\beta) \\ \dot{Y} = V\sin(\psi+\beta) \\ \dot{\psi} = \dfrac{V\cos(\beta)}{l_f+l_r}(\tan(\delta_f)-\tan(\delta_r)) \end{cases}, \tag{2}$$

where $\dot{X}$ and $\dot{Y}$ are horizontal and vertical velocities, V is the velocity of the vehicle, and ψ is yaw angle. Yaw angle describes how much vehicle is rotated around the global *Z* axis. Parameters l_f and l_r are the lengths from the vehicle's centre of mass to the front and rear axles. The parameters δ_r and δ_f represent the rear and front steering angles, and β is vehicle's slip angle. [6, p. 26] In a kinematic bicycle model, the coordinates, dimensions, and direction of the vehicle are used for modelling.

Dynamic bicycle model

The dynamic 2-Degree-of-Freedom (2-DOF) bicycle model demonstrates the motion of a vehicle, accounting for its dynamic traits. This model provides a more comprehensive analysis than the basic kinematic model, requiring the consideration of more states and

parameters. A dynamic bicycle model can be described, for example, by a state-space model as:

$$\begin{bmatrix} \dot{y} \\ \ddot{y} \\ \dot{\psi} \\ \ddot{\psi} \end{bmatrix} = \begin{bmatrix} 0 & 1 & 0 & 0 \\ 0 & -\frac{2C_{\alpha f} + 2C_{\alpha r}}{mV_x} & 0 & -V_x - \frac{2C_{\alpha f} l_f - 2C_{\alpha r} l_r}{mV_x} \\ 0 & 0 & 0 & 1 \\ 0 & -\frac{2l_f C_{\alpha f} - 2l_r C_{\alpha r}}{I_z V_x} & 0 & -\frac{2l_f^2 C_{\alpha f} + 2l_r^2 C_{\alpha r}}{I_z V_x} \end{bmatrix} \begin{bmatrix} y \\ \dot{y} \\ \psi \\ \dot{\psi} \end{bmatrix} + \begin{bmatrix} 0 \\ \frac{2C_{\alpha f}}{m} \\ 0 \\ \frac{2l_f C_{\alpha f}}{I_z} \end{bmatrix} \delta. \quad (3)$$

In the state-space model, the parameters $C_{\alpha f}$ and $C_{\alpha r}$ represent the cornering stiffness values of the tires, while m is the mass of the vehicle. Additionally, l_f and l_r represent the distances from the front and rear axles to the vehicle's center of gravity, and V_x represents the longitudinal velocity of the vehicle. Variable I_z signifies the moment based on the z-axis. Parameter $\dot{y}$ is lateral velocity, $\ddot{y}$ denotes lateral acceleration, $\dot{\psi}$ and $\ddot{\psi}$ refer to yaw angular velocity and angular acceleration. The variable δ is the steering angle of the front wheel. [6, p. 30]

The dynamic model is more challenging to implement because, for instance, cornering stiffness values require identification and are specific to the vehicle, road surface, and tires. These stiffness values can be estimated using the Pacejka magic formula [10, p. 7]. Using a dynamic vehicle model may not be a robust way to model vehicles, as the model relies on the vehicle's mass and the tire-road friction coefficient μ [6, p. 31]. For example, weather conditions can influence the friction coefficient, causing variations in model parameters [11]. Moreover, a basic linear model does not function effectively when dealing with significant steering angles, because linearization is made using small angle approximation [6, p. 30]. In scenarios requiring substantial steering angles, an alternative tire model is necessary.

2.2 Controllers

The nonlinearity of a vehicle introduces challenges when it comes to steering control. Various controllers and controller design approaches are employed, yielding different results. Some controllers are straightforward to design and are suitable for various situations, specific speeds, and steering angles. On the other hand, certain aspects of controller design are more complex but offer greater utility and robustness compared to simple controllers. This chapter presents a few controllers used in literature to control a lateral motion of vehicle. All these controllers are based on feedback systems. In a feedback system, the measured output is fed back to the controller's input, according to which the controller tries to decrease the control error [12, pp. 33–34].

2.2.1 1-DOF PID-controller

The PID controller stands out as well-known and extensively utilized controller, characterized by its P, I, and D components. The P-term of the control component is proportional to the error, the I-term is proportional to the error of the integral and the D-term is proportional to the derivative of the error. Summing these terms gives the control function u. [9, p. 64] The block diagram of PID-controller is shown in the Figure 2.

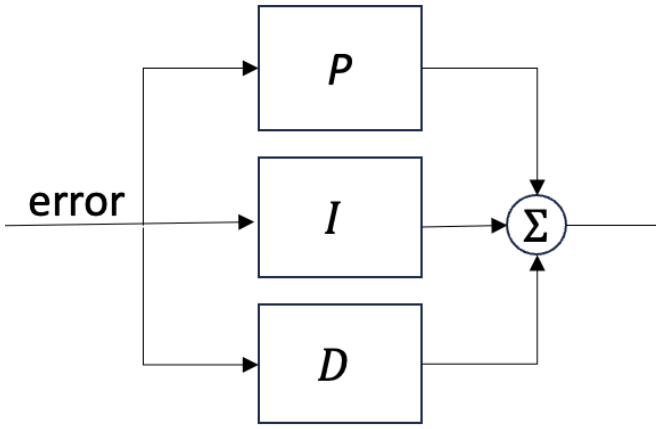

Figure 2. Block diagram of the PID-controller. [9, p. 71]

In Figure 2, the PID controller employs a control algorithm that generates a control signal by adding together the contributions of the Proportional (P), Integral (I), and Derivative (D) terms. While various alternatives have been devised, the illustration in Figure 2 represents the prevailing standard.

Terms of the PID-controller works in different ways. Figure 3 illustrates how the PID controller utilizes error information at different times.

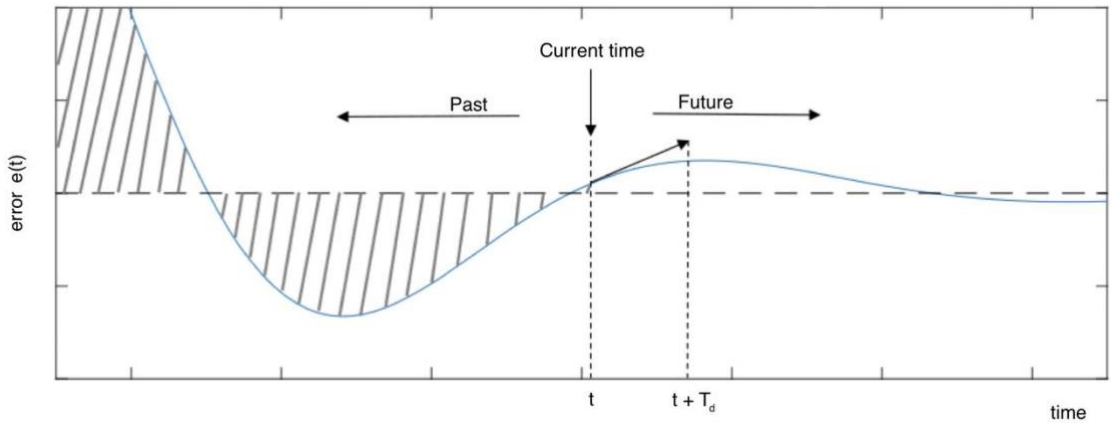

***Figure* 3.** PID controller uses past and present error information and predicts future by linear extrapolation. Edited from source [13].

In PID control, the P-term is static and responsible for real-time operation, providing control action in proportion to the current error. The proportional term does not guarantee accurate control by itself, as the error may not converge to zero. In contrast, the I-term employs integral values of past errors to primarily reduce control errors. The D-term, forecasts the future using derivatives, aiming to accelerate the controller's response and enhance closed-loop stability and damping of step response. [12, p. 64–69]

The operation of the 1-DOF-PID controller's output can be written as

$$u(t) = K_p e(t) + K_i \int_0^t e(\tau)\ d\tau + K_d \frac{de(t)}{dt}, e(t) = r(t) - y(t), \tag{4}$$

where K_p is the proportional gain, K_i and K_d are the integration and derivative gains respectively, and $u(t)$ is the control signal and $e(t)$ is error, $r(t)$ is reference value and $y(t)$ is output of the system. PID controller in discrete time can be represented by the equation

$$u(k) = K_p e(k) + K_i h \sum_{i=1}^{n} \left(\frac{e(i) + e(i-1)}{2}\right) + \frac{K_d}{h}\big(e(k) - e(k-1)\big), \tag{5}$$

where h is the sampling interval and k is an integer. In this thesis, discrete PID controller is used because the explored system is discrete. [14, pp. 193–195] The gains $K_i = K_p/T_i$ and $K_d = K_p T_d$ are used in this study, where T_i and T_d represent integration and derivative times.

PID-controllers are well-suited for LTI systems. Various combinations of PID terms are also available. For instance, you can use only the P-term, or you can use P-term and I-term together. The choice of terms depends on the system's dynamics and desired functionalities. [9, p. 87]

2.2.2 State-feedback control

The state of a dynamical system refers to how the system will evolve in the future. State-feedback controllers can be designed in several ways. In pole placement method, the main idea is to make use of the system's states and the matrixes ***A*** and ***B*** to position the eigenvalues of the closed-loop system. The eigenvalues are obtained from the equation

$$\det(\boldsymbol{\lambda I} - \boldsymbol{A}_{cl}) = 0, \tag{6}$$

where $\boldsymbol{\lambda}$ is eigenvalue vector, and $\boldsymbol{A}_{cl}$ is the dynamics matrix of a feedback system. Matrix ***I*** is identity matrix with the same dimensions as the matrix $\boldsymbol{A}_{cl}$. [15][16, pp. 175–178] State-feedback controller’s output is mathematically represented by (7)

$$\boldsymbol{u} = -\boldsymbol{K}\boldsymbol{x} + R_s r, \tag{7}$$

where $\boldsymbol{u}$ is control input, $\boldsymbol{x}$ is state-vector and $\boldsymbol{K}$ is a gain matrix where the dimensions depend on the number of variables to be controlled. Parameter R_s is the calibration value. [16, pp. 175–178]

The values within the gain matrix $\boldsymbol{K}$ have an impact on various properties of the system's step response, including overshoot, stability and settling time, which are desirable characteristics for the system's performance. Furthermore, the choice of parameters within the gain vector depends on the specific type of controller desired. [17, pp. 237–239]

2.2.3 Gain-scheduling

Nonlinearity of real-world systems makes control system design challenging. Traditional methods such as linear controllers may not work. Therefore, different approaches to the problem have been developed. Gain-scheduling is one example how to control nonlinear systems.

Gain-scheduling is a method that utilizes a set of linear controllers. These linear controllers are designed using linearized models derived from a nonlinear system model. Linearized models can be used in the design of a linear controller, such as PID controllers. [18, p. 1107]

A linear controller provided through gain-scheduling is an eligible choice because the design methods and control theory for linear control are well-established. In such cases, controller types like the ones mentioned above can be applied. [18, p. 1107]

2.3 Performance indicators

The quality of control can be measured and examined in different ways. There are various indicators that provide information on the performance of the system. In addition, performance of control can be investigated by simply measuring the error, control signal, setpoints and response of the system.

The two indicators used in this work are The Integral of Squared Error (ISE) and The Integral of Absolute Error (IAE). Both ISE and IAE describe the accumulation of error, which refers to the amount of area that accumulates between the error curve and the x-axis. ISE is calculated as follows

$$ISE = \int_0^T \big(e(t)\big)^2 \, dt, \tag{8}$$

where *T* signifies the time period which the error is being evaluated over. On the other hand, IAE is calculated

$$IAE = \int_0^T |e(t)|\ dt. \tag{9}$$

The primary distinction lies in the squaring of error values for ISE, which gives more weight to larger errors, while IAE treats all errors equally, regardless of their size. [19][20]

Time-weighted versions of IAE and ISE can also be expressed as Integral of Time multiplied Absolute Error (ITAE) and Integral of Time multiplied Squared Error (ITSE). ITAE is determined using

$$ITAE = \int_0^T t|e(t)|\ dt. \tag{10}$$

ITSE is calculated using

$$ITSE = \int_0^T t\big(e(t)\big)^2\ dt. \tag{11}$$

Time-weighted performance measures are used when system design values a short settling time and a reasonable percentage overshoot more than a short rise time and a high overshoot. [19][20]

In addition to the previous values, the rise time, settling time, overshoot and stability margins of the control system must be verified. Figure 4 illustrates settling time, overshoot and rise time.

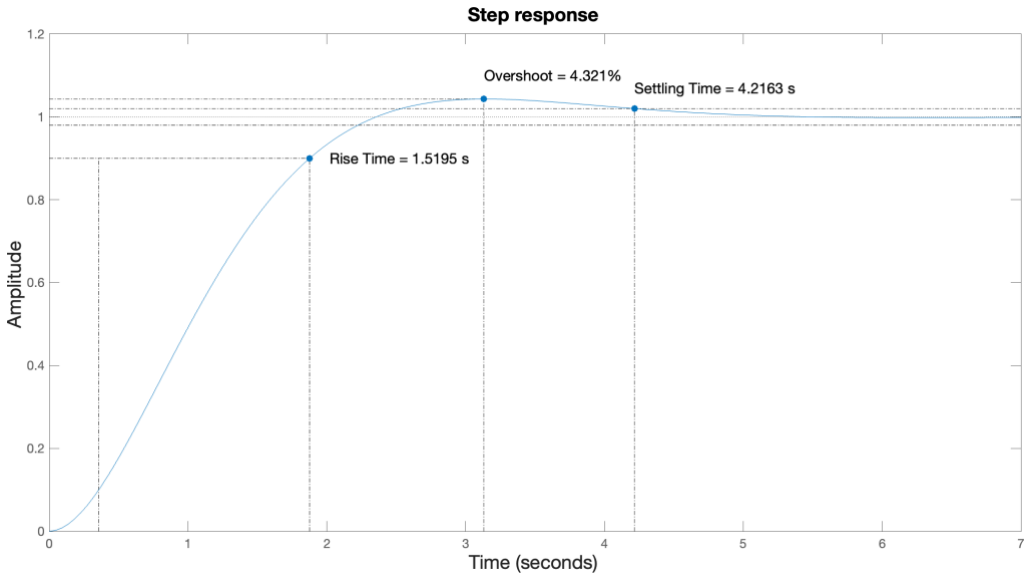

Figure 4. *Indicators of the step response.*

The rise time describes swiftness of the transient stage. Typically, this value is calculated as the time taken from ten to ninety percent of the final value of the response. Settling time describes the time it takes for the response to settle within a certain limit, for example within $\pm 2\%$ of the final value. [12, pp. 328–329] The overshoot describes how much the system response exceeds the target end value [21, pp. 474–478]. The characteristics of a system can also be studied using, for example, a Bode diagram. Figure 5 shows an example of a Bode diagram and stability margins.

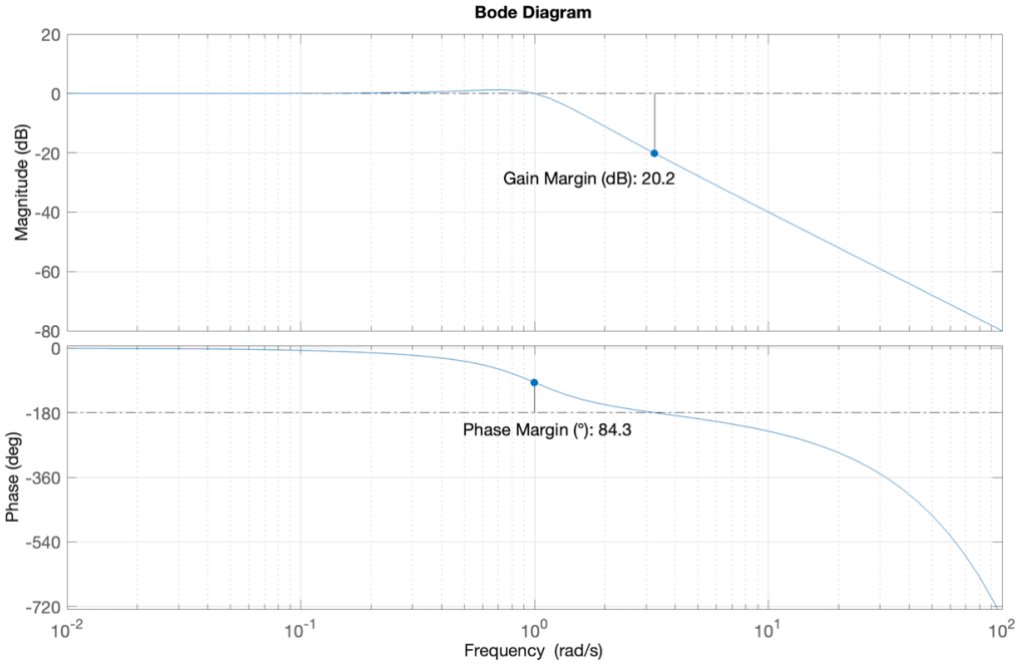

Figure 5. *Stability margins presented in the Bode diagram.*

With Bode diagram, for example, system's stability margins in frequency domain can be explored. [12, pp. 523–525]. Stability margins describes how much the values of gain, delay or phase can change before the system becomes critically stable [21, pp. 474–478].

3. STRUCTURE OF THE AUTOMATED VEHICLE

Autonomous driving needs complex systems to work. VTT Technical Research Centre of Finland researches autonomous driving, and in this thesis one of the automated vehicles, the Volkswagen Touareg, called "Martti", is used as a research vehicle. The automated vehicle has a wide range of different sensors and algorithms which are introduced in this chapter.

3.1 Architecture, Algorithms, Hardware and Sensors

The architecture of an autonomous vehicle includes many different algorithms, computers, and radars. Figure 6 shows the operational architecture of an automated car.

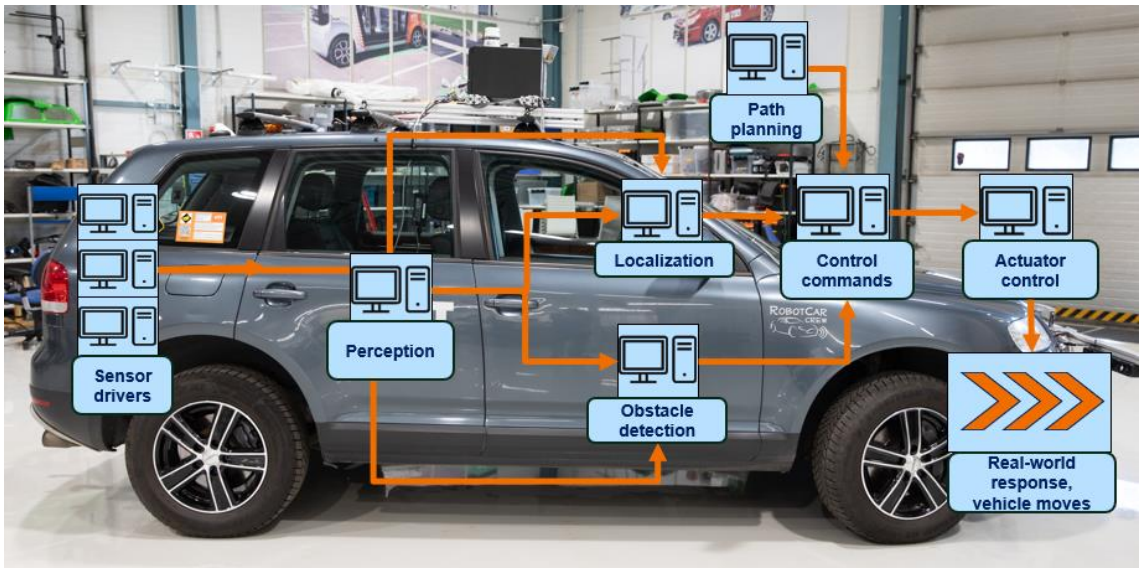

Figure 6. *Control architecture of self-driving car.*

The most relevant piece in Figure 6 for this work is the "Actuator control" block. It includes low-level control, such as actuator control algorithms. The actuator controller contains the control algorithms for the car's brake, steering wheel, and accelerator actuators. It also contains the motion control logic of the vehicle.

The actuator control receives control commands, such as the steering angle setpoints and the desired speed, from the control commands block. The control commands block combines location, obstacle, and route information, and provides control values to the actuator control block. In this case, only the control command and the actuator control blocks are considered.

The vehicle can be driven in different ways. For example, driving can be done using a pre-recorded route. In this work, the car is driven based on the position and direction of the car. This method is particularly convenient in this work, as it reduces the number of external error factors and provides more accurate information for the analysis of the control.

Autonomous vehicles require specific control, planning, and sensing algorithms to operate efficiently. The path controller is responsible for charting a course based on a pre-defined point-to-point route. It exploits real-time car position data and anticipates a point a short distance ahead, towards the direction of which the vehicle should steer at any given moment. By considering the car's current direction, velocity and curvature, the path controller calculates the necessary car curvature value. This value serves as the basis for determining essential parameters, including the required steering angle for the tires.

The vehicle controller considers various limiting factors, such as extreme steering angles and acceleration values. In addition to control functions, it incorporates logic for managing parameter adjustments needed for actions like braking. The vehicle controller also enforces constraints imposed by these limiting factors. An example of such constraints is the acceptable range for the steering angle of the tires, indicating that the tires cannot be turned arbitrarily but must remain within a specific angle range.

A wide range of sensors and equipment are needed to operate a car, but this thesis will only present the most relevant ones for control and steering. The most relevant data for steering are velocity, direction, and position of the vehicle. This data is obtained with three different instruments which are Odometry, Inertial Measurement Unit (IMU) and Global Navigation Satellite System (GNSS).

Odometry refers to the measurement and tracking of motion using a device's movement, such as wheels or treads. It is particularly important in the context of autonomous vehicles, where it helps predict the vehicle's position and motion based on the movements of its components. For example, in the case of a differential drive vehicle with two independently controlled wheels, odometry helps calculate the vehicle's trajectory and position. It plays a crucial role in navigation and tracking, especially in autonomous movements and distance measurement. [22]

Odometry is used in this work to measure the angle of the car's tyres, steering wheel, and the speed of the car. These are all read directly from the car's own Controller Area Network (CAN) to make the information as readable as possible. CAN is a

communication protocol that was originally designed for the automotive industry but is also widely used in other industries, for example, it’s commonly used in factories [23].

IMU is a device that measures and estimates the relative position, velocity, and acceleration of a moving vehicle. IMUs require real-time integration of data from sensors, for example accelerometers and gyroscopes, to determine the vehicle's motion relative to its initial frame. Modern IMUs can estimate a vehicle's 9-DOF. It consists of three primary components: accelerometer, gyroscope and magnetometer, each 3-DOF. Accelerometer measures acceleration, gyroscope measures the object's angular velocity or rotational movement, and magnetometer gives heading. [22][24]

GNSS is a widely used technology for determining precise location on Earth. It offers a three-dimensional position estimate, time and date information, and is accessible globally. Standard GNSS provides a position estimate an accuracy of about 20 meters. GNSS is widely used in various applications, such as vehicle navigation, outdoor activity and fleet tracking. Various techniques have been developed to increase the accuracy of GNSS. This work uses the RTK Fixed GNSS, which accuracy is between 1 to 3 centimetres. [22]

The control system in the test vehicle is distributed, which is why Data-Distributed System (DDS) is used for data transfer and communication between the different control units. DDS is a standardised way of communicating information in a distributed system. It is based on the "publisher/subscriber" method. In this method, each control unit can publish messages on the DDS network on a given topic and a control unit can subscribe messages from other units. In addition to the decentralisation of DDS, the system has the advantage of real time. [25]

3.2 Instrumentation constraints

When controlling any instrument, the accuracy of the measurement and other limitations of the instrumentation must be considered. Measurement inaccuracies and delays can cause problems and challenges for control. This subsection examines the sources of error and constraints of the test vehicle’s system.

The measurement and control system has been designed to be as delay-free as possible. However, delays can still occur due to factors like DDS, communication buses, and computation. Even every effort to minimize these delays are made, there will always be some delay in processing data from measurement to control value change. For instance, the car's speed and tire direction data come from the odometry, which is obtained from the car's own CAN bus. The control computer then calculates the

necessary steering commands. After this calculation is completed, the steering commands are transmitted over the bus to an actuator, which also introduces its own delay and time constant. There are many steps to the change in steering from a measured quantity in a single steering control cycle, during which uncertainty arises.

In addition to the delay, the control is constrained by the actuators. The servo motor used to steer the car in this application is not self-controlled but uses a proprietary interface and control system. Therefore, the readability and speed of the servo operation is not known of causing steering uncertainty.

One important factor that affects the quality of the control is the measurement. In a feedback system, control relies on measurements. Therefore, it is essential to consider factors that impact measurement accuracy within the control system. Measurement accuracy can be evaluated and analysed in various ways and multiple indicators can be used to assess the accuracy of measurements. However, in this specific application, many of these factors remain unknown. For instance, the sensor surface and measurement methods for the car's own speed and direction data are not well-documented.

In addition to the constraints mentioned above, certain types of sensors themselves pose constraints that need to be considered. IMUs are sensitive to measurement errors, which can lead to drift in orientation and position, which occur in the automotive environment often. External references, such as GNSS, are often used to correct these errors over time. [22]

4. VEHICLE TEST SCENARIOS WITH VARIOUS CONTROLLERS

This chapter focuses on the experimental section, which involves conducting tests on a test vehicle using various controllers. The aim is to use the results to examine the functionality of the control system, identify areas for improvement, and investigate the current characteristics of the car's steering.

4.1 Test methods

Three different control algorithms were implemented in the test vehicle: the P, -PI, - and PID controllers. These control types were used for practical measurements on the test track. The test track is depicted in Figure 7, with the x-axis representing longitude and the y-axis representing latitude coordinates.

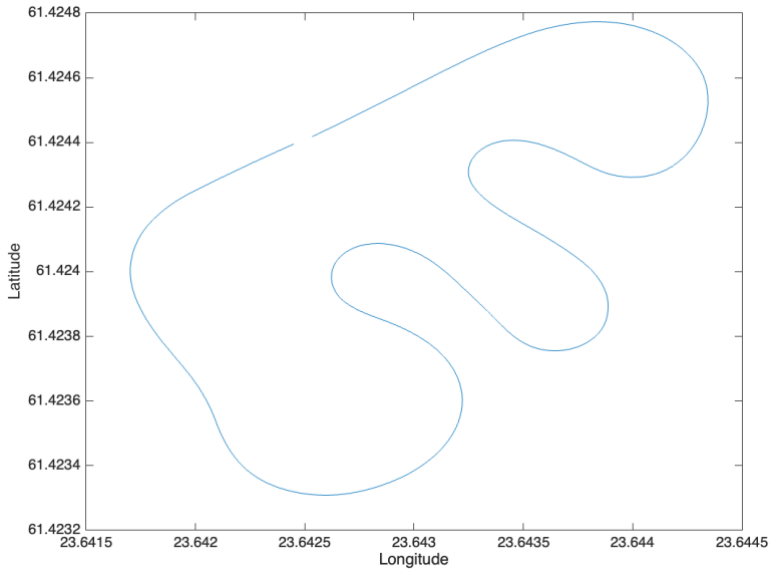

Figure 7. *Test track depicted in longitude and latitude coordinates.*

The test track includes a variety of bends to test the performance of the controllers in a wider range of situations. Each test is run at the same speed, 20 km/h, starting from the same point. At the beginning, the car is not at its target speed, but accelerates before the first corner. At the end of the route, the vehicle stops on its own.

The measurements have been made using XSENS MTi-630R IMU, Ublox ZED F9P RTK-GNSS and odometry. The measurement frequency for IMU is 100 Hz and for GNSS is 10 Hz. The odometry provides the angle between the tyres and the steering wheel and the vehicle speed at each moment. Steering control is achieved by adjusting the angular

velocity of the servomotor. Steering values in degrees of wheel angle are calculated by integrating the angular velocity of the wheel and tyres. The numerical integration was performed using the *cumtrapz* function in MATLAB software. Samples are collected at 10 ms intervals.

The controllers initially used contained the original gain values, which were later adjusted during the tests to enhance control performance. The structure of the controller is shown in the equation (5). The gain values of the controllers can be found in Table 1.

Table 1. Used PID gain values.

CONTROLLER	K_p	K_i	K_d
P	0.09	-	-
PI	0.08	0.03	-
PID	0.05	0.04	0.01

For each controller, the tire angle's target reference, the measured tire angle, timestamp and the steering control value were measured. The target reference value was obtained from the path planning algorithm.

4.2 Results

Figure 8 shows the measured values when driving with the P controller.

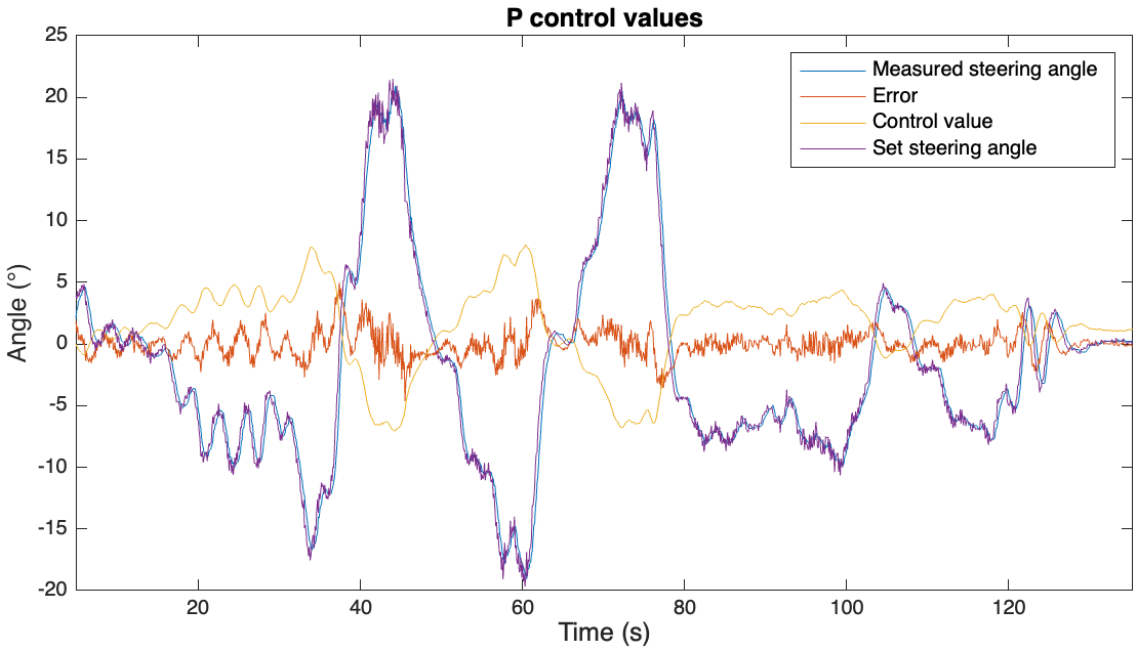

Figure 8. *Measured values when using P controller.*

The graph shows that the angle of the tyres oscillates, especially for small changes in the target reference. This is due to the relatively high value of gain required for larger curves, because with larger target reference changes, the oscillation is smaller. It is also typical for P control that the control error never reaches zero, and the control can remain oscillating.

A delay was determined between the reference value and the measured value. This delay represents the time taken by the control system to reach the target reference. For different controllers, the delay varied between 0.25 and 0.30 seconds. In other words, the measured values are delayed by a certain amount relative to the target reference. Delays increase the value of the error.

Oscillation is not only caused by the control but is also heavily influenced by the routing algorithm. The current P controller keeps up relatively well with changes in set values, but due to delay and interference, it does not reach the full target reference. The graph also shows how much the target reference oscillate; this degrades the control.

The same measurements were also repeated with the PI controller. The results can be seen in Figure 9.

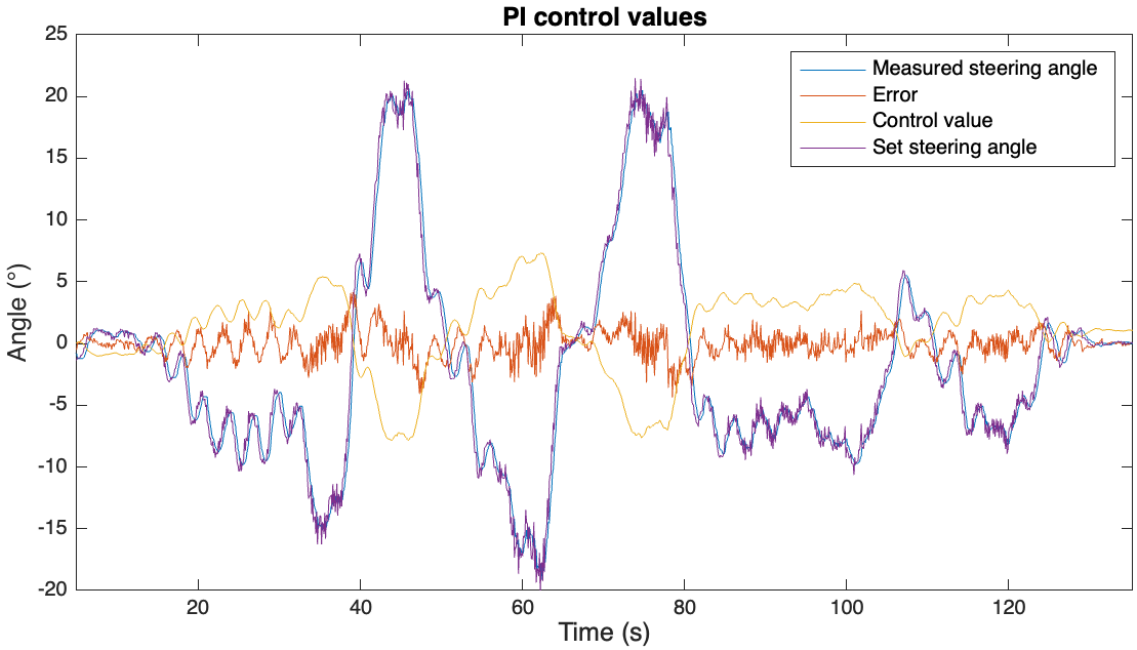

Figure 9. *Measured values when using PI controller.*

Compared to the P controller, the PI controller mitigates error at lower setpoints. The additional oscillation that occurs is smaller compared to the P controller. From the graph, it can be concluded that the PI controller performs better in this application. The third test was performed with a PID controller, the measurement results of which are shown in Figure 10.

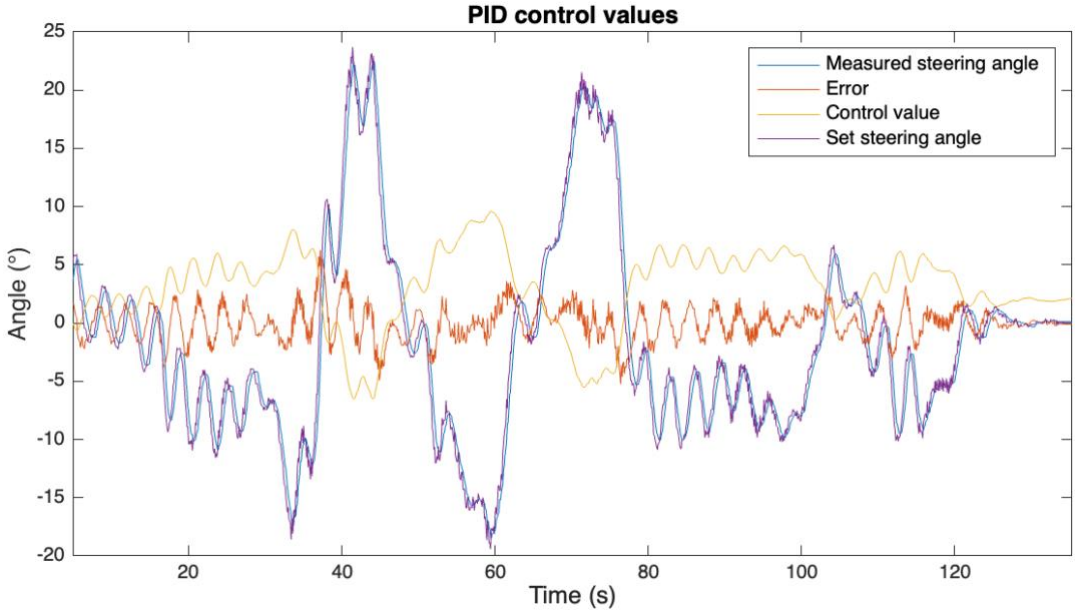

Figure 10. *Measured values when using PID controller.*

With a PID controller, the error, setpoints and response oscillate strongly, because the D-term of the PID controller acts as a derivator that reacts strongly to spurious errors and noise. Due to the excessive gain of the D-term in this measurement, the oscillation was too strong.

In addition to these measurements, the performance and quality of controllers can be compared in several ways. Figure 11 shows the IAEs and ISEs for all three controllers.

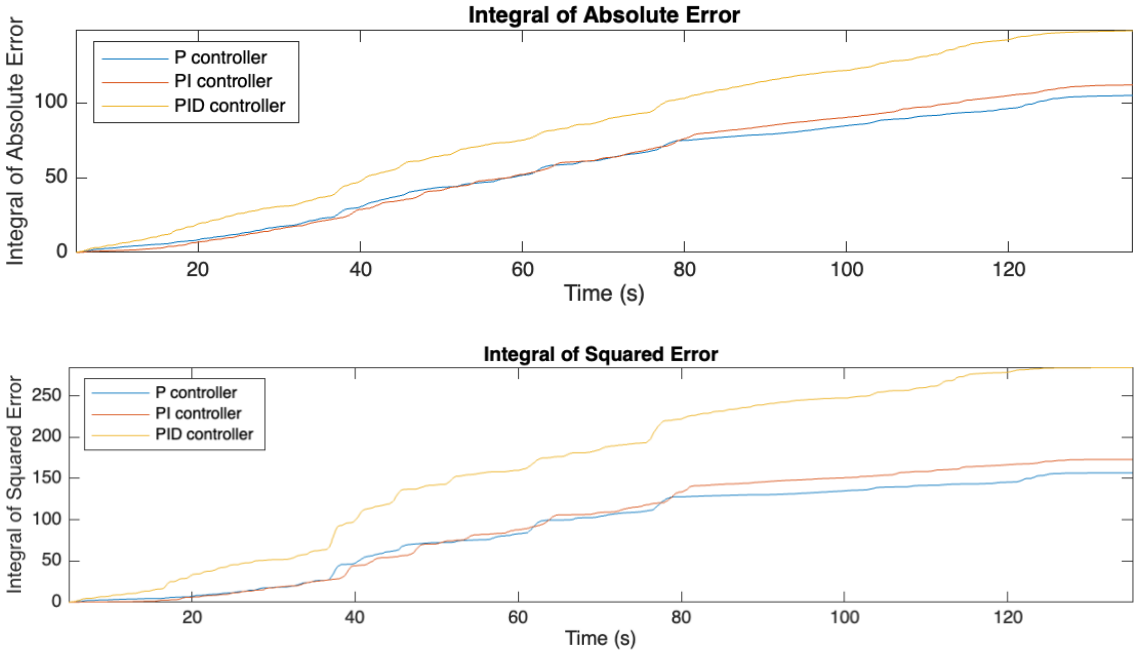

Figure 11. *IAEs and ISEs of the controllers.*

The graph shows that the P and PI controllers have the smallest errors. Towards the end, however, the absolute error of the P controller is lower than that of the PI controller,

so when looking at the error, the final value of the P controller is better, but the error accumulation of the PI controller is smoother. The first five seconds have been excluded from the calculations because the initial values distorted the results.

From the graph, it can be observed that the accumulation of square error slows down around the 80-second mark for both P and PI controllers. This suggests that the error is relatively small compared to the error accumulation of a PID controller, which exhibits a higher growth rate. In comparison to the computed values of IAE, the accumulation of ISE is more gradual. Relative to the travelled path, it is noticeable that the largest errors occur in the early part of the trajectory, particularly around radical turns. Towards the end, the error levels off as the turns become gentler, except when using a PID controller. For both IAE and ISE, there is a large increase at 70-80 seconds for all regulators, as the target reference changes significantly at that time.

Time-weighted versions of the IAE and ISE are not used in this work because the target reference values change frequently. Therefore, time weighted ratios may distort the calculations and thus do not add value to the calculation and to the comparison of regulators.

In addition to the steering measurements, the position of the vehicle was measured. For the most part, the vehicle stayed on track, but there was some oversteer on all controllers, especially on steep bends. Figure 12 shows the route taken by the vehicle and the recorded route.

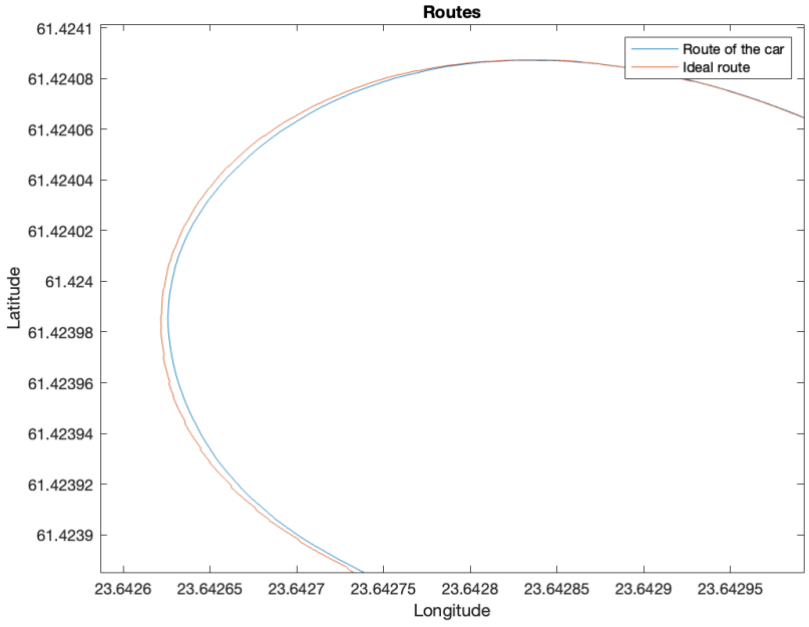

Figure 12. *Part of the ideal and vehicle-driven route.*

The picture shows the vehicle swerving around a steep bend. This is due to an excessive gain value and the route tracking algorithm. In the route-following algorithm, the correction is due to a too high a lookahead and gain values. The lookahead term indicates the reference point used in steer calculations along the upcoming route. That is, at a turn, the lookahead is slightly above the right-angle value, which causes a correction.

The distance between the recorded route and the driven route was calculated. The standard deviations and average values of the route deviation are shown in Table 2.

Table 2. Standard deviation and average values of the route deviation.

	Average value of the route deviation (m)	Standard deviation
P	0.2859	0.2037
PI	0.2516	0.1189
PID	0.2858	0.1750

When comparing the averages, the car stayed best on its route with the PI controller and worst with the P and PID controllers. In addition, the PI control had the lowest standard deviation.

5. CONCLUSIONS

The experiment aimed to assess the performance of three different controllers on a specific test track under varying conditions, and the results aligned with expectations. Notably, the nonlinearity in the vehicle's steering system had a clear influence on the outcomes.

When dealing with significant changes in the steering angle, both the P and PI controllers demonstrated good performance. The P controller exhibited minor oscillations, even with small set values, while the PI controller effectively mitigated these oscillations. However, the PID controller consistently exhibited oscillatory behaviour across all settings.

The lowest final IAE and ISE values was produced by the P controller, while the highest final values was yielded by the PID controller when the accumulated error was evaluated. The differences in errors between the P and PI controllers became most apparent toward the end of the testing. Furthermore, when it came to route deviations, the PI controller outperformed the P and PID controllers. Consequently, the best results were achieved with the P and PI controllers, with the PI controller delivering smoother performance and fewer oscillations.

It is important to acknowledge that the controllers used in the experiment are linear with constant co-effs, which may not give good results. For example, larger changes in the steering angle exhibited fewer oscillations compared to smaller ones. Additionally, when tested at higher speeds with identical gain values, the system became prone to instability. Therefore, enhancing the control system, possibly through strategies like gain-scheduling and a more precise model, could lead to overall performance improvements.

The thesis presented a couple of different types of controllers and a vehicle modelling approaches. The work as a whole was successful, and information about the control system of the vehicle studied was obtained. The data collected was used to identify various areas for improvement and development of the control system of the vehicle, which was one of the motivations for doing this work. In the future, this work could be used to explore which methods could be used to modify and improve the vehicle's steering control system.

REFERENCES

[1] M. Rasib, M. A. Butt, S. Khalid, S. Abid, F. Raiz, Jabbar S, et al. Are Self-Driving Vehicles Ready to Launch? An Insight into Steering Control in Autonomous Self-Driving Vehicles, Mathematical problems in engineering, 2021.

[2] C. Hu, Y. Qin, H. Cao, X. Song, K. Jiang, J. J. Rath, et al. Lane keeping of autonomous vehicles based on differential steering with adaptive multivariable super-twisting control, Mechanical systems and signal processing, 2019.

[3] S. Cheng, L. Li, H.Q. Guo, Z. G. Chen, P. Song, Longitudinal Collision Avoidance and Lateral Stability Adaptive Control System Based on MPC of Autonomous Vehicles, IEEE transactions on intelligent transportation systems, 2020.

[4] X. Huang, H. Zhang, G. Zhang, J. Wang, Robust Weighted Gain-Scheduling H∞ Vehicle Lateral Motion Control With Considerations of Steering System Backlash-Type Hysteresis. IEEE transactions on control systems technology, 2014.

[5] G. Han, W. Fu, W. Wang, Z. Wu, The Lateral Tracking Control for the Intelligent Vehicle Based on Adaptive PID Neural Network. Sensors (Basel, Switzerland). 2017;17(6):1244-.

[6] R. Rajamani, Vehicle Dynamics and Control. 2. Aufl. New York, NY: Springer Nature, 2011.

[7] E.W. Weisstein, CRC Concise Encyclopedia of Mathematics. 2nd ed. London: Chapman and Hall/CRC; 2002.

[8] E. Hendricks, O. Jannerup, P.H. Sørensen, Linear Systems Control: Deterministic and Stochastic Methods. 1. Aufl. Berlin, Heidelberg: Springer-Verlag; 2008.

[9] K.J. Åström, T. Hägglund, Advanced PID control, Research Triangle Park, NC: ISA, 2006.

[10] H. Pacejka, I.J.M Besselink, Tire and Vehicle Dynamics (3rd Edition). 3rd ed. Oxford: Elsevier; 2012.

[11] H. Zhu, Y. Tian, W. Zhang, Studies of Tire Frictional Characteristics on the Snowy Road, SAE Technical Papers, 2023.

[12] R.C. Dorf, R.H. Bishop, Modern control systems, Thirteenth edition. Harlow: Pearson, 2017.

[13] V.-P. Pyrhönen, Johdatus systeemien hallintaan: Lecture 6, Tampere University, Tampere, 2023.

[14] R.C. Panda, Introduction to PID controllers : theory, tuning and application to frontiers area, Rijeka, Crotia: IntechOpen, 2012.

[15] Promode Kumar Saikia, Linear Algebra, 2/e, 2nd Edition, Pearson Education India, 2014.

[16] K.J. Åström, R.M. Murray, Feedback Systems: An Introduction for Scientists and Engineers, Princeton, NJ: Princeton University Press, 2010.

[17] Chen, C. Chi-Tsong, C. Chi-Tsong, Linear system theory and design. 3rd ed. New York: Oxford University Press, 1999.

[18] W.K. Chen, Electrical Engineering Handbook, 1st ed. San Diego: Elsevier, 2004.

[19] W.C. Schultz, V.C. Rideout, Control system performance measures: Past, present, and future. IRE transactions on automatic control, 1961.

[20] S.K. Bhattacharya, Control systems engineering. 3rd. ed. New Delhi, India: Pearson, 2013.

[21] K. Ogata, Modern control engineering. 5th ed. Upper Saddle River (NJ): Pearson, 2010.

[22] M. Jenkin, J. Dudek, Inertial Sensors, GPS, and Odometry. Springer Handbook of Robotics. 2008. p. 477–90.

[23] Copperhill Technologies Corporation, "A Brief Introduction to Controller Area Network," [Online]. Available: https://copperhilltech.com/a-brief-introduction-to-controller-area-network/.

[24] S.B. Farahan, J.J.M. Machado, F.G. de Almeida, J.M. Tavares, 9-DOF IMU-Based Attitude and Heading Estimation Using an Extended Kalman Filter with Bias Consideration. Sensors (Basel, Switzerland). 2022.

[25] Pardo-Castellote G. OMG Data-Distribution Service: architectural overview. In: 23rd International Conference on Distributed Computing Systems Workshops, 2003 Proceedings. IEEE, 2003. p. 200–6.